Hindawi Publishing Corporation
Discrete Dynamics in Nature and Society
Volume 2015, Article ID 682140, 7 pages
http://dx.doi.org/10.1155/2015/682140

Research Article

A Parallel Spectral Element Method for Fractional Lorenz System

Yanhui Su

College of Mathematics and Computer Science, Fuzhou University, Fuzhou 350108, China

Correspondence should be addressed to Yanhui Su; suyh@fzu.edu.cn

Received 21 September 2014; Revised 4 April 2015; Accepted 7 April 2015

Academic Editor: Daniele Fournier-Prunaret

Copyright © 2015 Yanhui Su. This is an open access article distributed under the Creative Commons Attribution License, which permits unrestricted use, distribution, and reproduction in any medium, provided the original work is properly cited.

We provide a parallel spectral element method for the fractional Lorenz system numerically. The detailed construction and implementation of the method are presented. Thanks to the spectral accuracy of the presented method, the storage requirement due to the "global time dependence" can be considerably relaxed. Also, the parareal method combining spectral element method reduces the computing time greatly. Finally, we have tested the chaotic behaviors of fractional Lorenz system. Our numerical results are in excellent agreement with the results from other numerical methods.

1. Introduction

In 1963, Lorenz [1] attempted to set up a (much simpler and easier-to-analyze) system of differential equations that would explain some of the unpredictable behavior of the weather. The classical Lorenz system is

$$\begin{aligned} x' &= \sigma(y - x), \\ y' &= \rho x - y - xz, \\ z' &= xy - bz, \end{aligned} \tag{1}$$

where all three parameters, ρ, σ, b, are assumed to be positive, and moreover, $\sigma > b+1$. Lorenz made an important discovery that all nonequilibrium solutions tend eventually to the same complicated set, the Lorenz attractor. The behavior of the chaotic system is one of the most important subjects in modern mathematics.

In [2], I. Grigorenko and E. Grigorenko generalized the Lorenz system to the fractional case by replacing the usual derivatives by the fractional one and found some interesting chaotic behaviors of fractional Lorenz system. This generation is natural. As we know, fractional derivatives play a more and more important role in modern sciences. They appear in the investigation of transport dynamics in complex systems which are characterized by the anomalous diffusion and nonexponential patterns [3]. It has been shown that many important physical and biological systems can be described by fractional differential equations (see [3–6], etc.). This has led to some investigations on the theoretical analysis and scientifical computation of the fractional differential equations in recent years (for details see [7–13] and the references therein). However, the fact that the fractional derivative is a nonlocal operator makes the results of fractional calculus in many respects far from complete.

First, let us recall that, for $0 < \alpha < 1$ and $f(t)$ defined on the interval $[a, b]$, the (Caputo) fractional derivative is defined as

$${}_aD_t^\alpha f(t) = \frac{1}{\Gamma(1-\alpha)} \int_a^t \frac{f'(\tau)}{(t-\tau)^\alpha} d\tau, \quad t \in [a, b], \tag{2}$$

where, $\Gamma(\cdot)$ is the Gamma function. And for simplicity, we denote $c(\alpha) = 1/\Gamma(1-\alpha)$. Thus, the fractional generalization of the Lorenz system is

$$\begin{aligned} {}_0D_t^\alpha x &= \sigma(y - x), \\ {}_0D_t^\beta y &= \rho x - y - xz^r, \\ {}_0D_t^\gamma z &= xy - bz, \end{aligned} \tag{3}$$

where $0 < \alpha, \beta, \gamma \leq 1$, and $r \geq 1$ is an integer. In [2], the authors pointed out that the system can have an effective

noninteger dimension Σ defined as the sum of the orders of all involved derivatives. They found that the system with $\Sigma < 3$ can also exhibit chaotic behavior. Furthermore, a striking finding is that there is a critical value of the effective dimension Σ_{cr}, under which the system undergoes a transition from chaotic daynamics to regular one.

The numerical scheme of [2] is based on the linearization of system (3), on each step of integration and iterative application of the exact solution of linear fractional differential equations. Also, homotopy methods to solve the (fractional) Lorenz system were proposed in [14, 15]. It has been known that the feature of the fractional derivatives makes the design of accurate and fast methods difficult. Unlike the integer derivatives, which are local in the sense that the derivative of a function at a certain point depends only on the function in the vicinity of this point, presence of the integral in the noninteger order derivatives makes the problem global. This means that the solution at a time t_k depends on the solutions at all previous time levels $t < t_k$. The fact that all previous solutions have to be saved to compute the solution at the current time level would make the storage very expensive if low-order methods are employed for temporal discretization. Thus, it is very desirable to use high-order methods for efficient computations of the numerical solution of this kind of problem. Among the high-order methods, spectral methods are known to be very useful for their exponential rate of convergence, which is also demonstrated for solving fractional differential equations [8, 9]. Thanks to the spectral accuracy, the storage requirement due to the "global time dependence" can be considerably relaxed. However, a drawback of the spectral method is also well-known; that is, the matrix associated with the spectral method is full and the computational cost grows more quickly than that of a low-order method. Thus for long integration it is desirable to combine the spectral method with domain decomposition techniques to avoid using a single high-degree polynomial (see [16] for details). This motivates us to consider the parallel spectral element method, since, as compared to a low-order method, this method needs fewer grid points to produce highly accurate solutions, and, furthermore, the parallel method reduces the computing time greatly.

This paper is organized as follows. In Section 2, we construct and implement the parallel spectral element schema for the numerical solution of the fractional Lorenz system. In Section 3, we have tested the chaotic behavior of fractional Lorenz system using our numerical method. The numerical results are in excellent agreement with the results from other numerical methods. Finally, Section 4 includes some concluding remarks.

2. The Implementation of the Parallel Spectral Element Method

In this section, we implement the parallel spectral element method for fractional Lorenz system (3). First, we divide the interval $I = [0, T]$ into M subintervals $I_m = [t_{m-1}, t_m]$, $m = 1, \ldots, M$. The length of each subinterval is $\Delta t = T/M$, and $t_m = m\Delta t$, $m = 0, 1, \ldots, M$. According to this partition, (3) is divided into the following system of M equations:

$$
\begin{aligned}
{}_{t_{m-1}}D_t^{\alpha} x_m &= \sigma\left(y_m - x_m\right) - c\left(\alpha\right) \sum_{k=1}^{m-1} \int_{t_{k-1}}^{t_k} \frac{x_k'\left(\tau\right)}{\left(t-\tau\right)^{\alpha}} d\tau, \\
{}_{t_{m-1}}D_t^{\beta} y_m &= \rho x_m - y_m - x_m z_m^r \\
&\quad - c\left(\beta\right) \sum_{k=1}^{m-1} \int_{t_{k-1}}^{t_k} \frac{y_k'\left(\tau\right)}{\left(t-\tau\right)^{\beta}} d\tau, \\
{}_{t_{m-1}}D_t^{\gamma} z_m &= x_m y_m - b z_m - c\left(\gamma\right) \sum_{k=1}^{m-1} \int_{t_{k-1}}^{t_k} \frac{z_k'\left(\tau\right)}{\left(t-\tau\right)^{\gamma}} d\tau, \\
&\qquad\qquad t \in I_m,
\end{aligned}
\tag{4}
$$

with $x_m = x|_{I_m}$, $y_m = y|_{I_m}$, and $z_m = z|_{I_m}$, $m = 1, 2, \ldots, M$. Let $\mathbf{X}_m = \{x_m, y_m, z_m\}$; then the solution of (4) can be expressed by the solvers S_m as follows:

$$
\mathbf{X}_m\left(t\right) = S_m\left(\mathbf{X}_1, \ldots, \mathbf{X}_{m-1}\right), \quad t \in I_m. \tag{5}
$$

In most cases S_m is not realizable and needs to be approximated.

The main idea of the parallel method consists of two steps. First, design two families of discrete solvers, fine solver $\mathcal{F}_m$ and coarse solver $\mathcal{G}_m$, to approximate S_m. The fine approximate solver $\mathcal{F}_m$ is defined by the spectral collocation method with polynomial degree of N:

$$
\mathbf{U}_m\left(t\right) = \mathcal{F}_m\left(\mathbf{U}_1, \ldots, \mathbf{U}_{m-1}\right), \tag{6}
$$

with the polynomial $\mathbf{U}_m = (U_m, V_m, W_m)$ of degree N. The coarse solver operator $\mathcal{G}_m$ is defined in the same way, using polynomials of a lower degree $\widetilde{N} < N$. Second, set up the iteration:

$$
\begin{aligned}
\mathbf{U}_m^k\left(t\right) &= \mathcal{G}_m\left(\mathbf{U}_1^k, \ldots, \mathbf{U}_{m-1}^k\right) + \mathcal{F}_m\left(\mathbf{U}_1^{k-1}, \ldots, \mathbf{U}_{m-1}^{k-1}\right) \\
&\quad - \mathcal{G}_m\left(\mathbf{U}_1^{k-1}, \ldots, \mathbf{U}_{m-1}^{k-1}\right), \quad k \geq 1,
\end{aligned}
\tag{7}
$$

with the initial value

$$
\mathbf{U}_m^0\left(t\right) = \mathcal{G}_m\left(\mathbf{U}_1^0, \ldots, \mathbf{U}_{m-1}^0\right), \tag{8}
$$

where subscript m refers to the element number, subscript k refers to the iteration number, and the polynomial $\mathbf{U}_m^k = (U_m^k, V_m^k, W_m^k)$ is the approximate solution of $\mathbf{X}_m$ at the time interval I_m. The parallel scheme can be seen as the predictor-corrector method, with the predictor $\mathcal{G}_m(\mathbf{U}_1^k, \ldots, \mathbf{U}_{m-1}^k)$ and the corrector $\mathcal{C}_m =: \mathcal{F}_m(\mathbf{U}_1^{k-1}, \ldots, \mathbf{U}_{m-1}^{k-1}) - \mathcal{G}_m(\mathbf{U}_1^{k-1}, \ldots, \mathbf{U}_{m-1}^{k-1})$. The key point of the parallel method is that the corrector $\mathcal{C}_m$ can be computed in parallel for $1 \leq m \leq M$. The predictor term $\mathcal{G}_m(\mathbf{U}_1^k, \ldots, \mathbf{U}_{m-1}^k)$ in (7) must be computed sequentially, but this is relatively cheap if $\widetilde{N}$ is small compared to N. Thus, provided the iteration converges rapidly, we can use multiple processors to obtain the high-accuracy solution

in a small multiple of the time needed to compute a low-accuracy solution.

Now we begin to describe the fine approximate solver $\mathscr{F}_m$. We first define $\mathscr{P}_N$ as the polynomial space of degree less than or equal to N. We denote by $J_N^{\alpha,\beta}(x)$, $x \in [-1,1]$, the Jacobi polynomial of degree N with respect to the weight function $\omega^{\alpha,\beta}(x) = (1-x)^\alpha(1+x)^\beta$, $-1 < \alpha, \beta < 1$. Let $x_i^{\alpha,\beta}$ be the points of the Gauss-Labatto-Jacobi (GJ) quadrature formula, defined by

$$J_{N+1}^{\alpha,\beta}\left(x_i^{\alpha,\beta}\right) = 0, \quad i = 0, \ldots, N, \tag{9}$$

arranged by increasing order: $x_0^{\alpha,\beta} < x_1^{\alpha,\beta} < \cdots < x_N^{\alpha,\beta}$. The associated weights of the GLJ quadrature formula are denoted by $\omega_i^{\alpha,\beta}$, $0 \le i \le N$. Particularly, let ξ_m^i be the Gauss-Labatto-Legendre (GLL) points on the interval I_m.

Thus, the spectral collocation method for fractional Lorenz system (3) on each subinterval I_m is to find $U_m(t), V_m(t), W_m(t) \in \mathscr{P}_N(I_m)$, such that for all $0 \le i \le N$

$$\begin{aligned}
&{}_{t_{m-1}}D_t^\alpha U_m\left(\xi_m^i\right) + \sigma U_m\left(\xi_m^i\right) - \sigma V_m\left(\xi_m^i\right) \\
&\quad = -c(\alpha)\sum_{k=1}^{m-1}\int_{t_{k-1}}^{t_k}\frac{U_k'(\tau)\,d\tau}{\left(\xi_m^i-\tau\right)^\alpha}, \\
&{}_{t_{m-1}}D_t^\beta V_m\left(\xi_m^i\right) - \rho U_m\left(\xi_m^i\right) + V_m\left(\xi_m^i\right) \\
&\quad + U_m\left(\xi_m^i\right)\left(W_m\left(\xi_m^i\right)\right)^r \\
&\quad = -c(\beta)\sum_{k=1}^{m-1}\int_{t_{k-1}}^{t_k}\frac{V_k'(\tau)\,d\tau}{\left(\xi_m^i-\tau\right)^\beta}, \\
&{}_{t_{m-1}}D_t^\gamma W_m\left(\xi_n^i\right) + bW_m\left(\xi_n^i\right) - U_m\left(\xi_n^i\right)V_m\left(\xi_n^i\right) \\
&\quad = -c(\gamma)\sum_{k=1}^{m-1}\int_{t_{k-1}}^{t_k}\frac{W_k'(\tau)\,d\tau}{\left(\xi_m^i-\tau\right)^\gamma}.
\end{aligned} \tag{10}$$

For the nonlinear problem (10), we choose to use the Lagrangian polynomials as a basis of the approximation spaces. Let $\{h_m^i(t) \mid i = 0, 1, \ldots, N\}$ be the Lagrangian polynomials associated with the points $\{\xi_m^i \mid i = 0, 1, \ldots, N\}$. That is, $h_m^i(t) \in \mathscr{P}_N(I_m)$ such that $h_m^i(\xi_m^k) = \delta_{ik}$, where δ denotes the Kronecker function. It is seen that the set $\{h_m^i(t); i = 0, \ldots, N\}$ forms a basis of $\mathscr{P}_N(I_m)$:

$$P_N(I_m) = \operatorname{span}\left\{h_m^i(t),\ i = 0, \ldots, N\right\}. \tag{11}$$

By expressing U_m, V_m, and W_m and all nonlinear term $(W_m(t))^r$ in this basis,

$$\begin{aligned}
U_m(t) &= \sum_{i=0}^N u_m^i h_m^i(t), \\
V_m(t) &= \sum_{i=0}^N v_m^i h_m^i(t), \\
W_m(t) &= \sum_{i=0}^N w_m^i h_m^i(t), \\
\left(W_m(t)\right)^r &= \sum_{i=0}^N \left(w_m^i\right)^r h_m^i(t).
\end{aligned} \tag{12}$$

We arrive at the matrix statement of (10):

$$\begin{aligned}
A_m^1\mathbf{u}_m + \sigma\mathbf{u}_m - \sigma\mathbf{v}_m &= \sum_{k=1}^{m-1} B_{m,k}^1\mathbf{u}_k, \\
A_m^2\mathbf{v}_m - \rho\mathbf{u}_m + \mathbf{v}_m + \mathbf{u}_m * \left(\mathbf{w}_m\right)^r &= \sum_{k=1}^{m-1} B_{m,k}^2\mathbf{v}_k, \\
A_m^3\mathbf{w}_m + b\mathbf{w}_m - \mathbf{u}_m\mathbf{v}_m &= \sum_{k=1}^{m-1} B_{m,k}^3\mathbf{w}_k,
\end{aligned} \tag{13}$$

where $\mathbf{u}_m = (u_m^i)_{(N+1)}$, $\mathbf{v}_m = (v_m^i)_{(N+1)}$, and $\mathbf{w}_m = (w_m^i)_{(N+1)}$ are the unknown vectors. $*$ is acting on two vectors $(\mathbf{u} * \mathbf{v})_i = \mathbf{u}_i * \mathbf{v}_i$. The matrices A_m^1, A_m^2, A_m^3, $B_{m,k}^1$, $B_{m,k}^2$, and $B_{m,k}^3$ are $(N+1)\times(N+1)$ matrices. They are computed as follows:

$$\begin{aligned}
A_m^1(i,j) &= c(\alpha)\int_{t_{m-1}}^{\xi_m^i}\frac{h_m^{j\prime}(\tau)}{\left(\xi_m^i-\tau\right)^\alpha}d\tau, \\
B_{m,k}^1(i,j) &= -c(\alpha)\int_{t_{k-1}}^{t_k}\frac{h_k^{j\prime}(\tau)}{\left(\xi_m^i-\tau\right)^\alpha}d\tau, \\
A_m^2(i,j) &= c(\beta)\int_{t_{m-1}}^{\xi_m^i}\frac{h_m^{j\prime}(\tau)}{\left(\xi_m^i-\tau\right)^\beta}d\tau, \\
B_{m,k}^2(i,j) &= -c(\beta)\int_{t_{k-1}}^{t_k}\frac{h_k^{j\prime}(\tau)}{\left(\xi_m^i-\tau\right)^\beta}d\tau, \\
A_m^3(i,j) &= c(\gamma)\int_{t_{m-1}}^{\xi_m^i}\frac{h_m^{j\prime}(\tau)}{\left(\xi_m^i-\tau\right)^\gamma}d\tau, \\
B_{m,k}^3(i,j) &= -c(\gamma)\int_{t_{k-1}}^{t_k}\frac{h_k^{j\prime}(\tau)}{\left(\xi_m^i-\tau\right)^\gamma}d\tau.
\end{aligned} \tag{14}$$

We are now led to compute the integrals $\int_{t_{m-1}}^{\xi_m^i}(h_m^{j\prime}(\tau)/(\xi_m^i-\tau)^\alpha)d\tau$ and $\int_{t_{k-1}}^{t_k}(h_k^{j\prime}(\tau)/(\xi_m^i-\tau)^\alpha)d\tau$ one by one.

For the first one, we employ Gauss-type quadrature to calculate it. It is well-known that the numerical quadrature

$$\int_{-1}^1 u(t)(1-t)^{-\alpha}\,dt \simeq \sum_{k=0}^N u\left(x_k^{-\alpha,0}\right)\omega_k^{-\alpha,0} \tag{15}$$

is exact for all functions u such that $u \in P_{2N-1}(-1,1)$. As a result, by the linear variable transformation

$$\tau(\theta) = \frac{\xi_m^i - t_{m-1}}{2}\theta + \frac{\xi_m^i + t_{m-1}}{2}, \quad \theta \in [-1,1], \tag{16}$$

it holds

$$\begin{aligned}\int_{t_{m-1}}^{\xi_m^i} \frac{h_m^{j\prime}(\tau)}{(\xi_m^i-\tau)^\alpha}d\tau &= \left(\frac{\xi_m^i-t_{m-1}}{2}\right)^{1-\alpha}\int_{-1}^{1}(1-\theta)^{-\alpha}h_m^{j\prime}(\tau(\theta))\,d\theta \\ &= \left(\frac{\xi_m^i-t_{m-1}}{2}\right)^{1-\alpha}\sum_{k=0}^{N}h_m^{j\prime}\left(\tau\left(x_k^{-\alpha,0}\right)\right)\omega_k^{-\alpha,0},\end{aligned} \tag{17}$$

since $h_m^{j\prime}(\tau(\theta)) \in P_{2N-1}(I)$ for all $j = 0, 1, \ldots, N$.

For the second one, it is important to point out that the Gauss-type quadrature fails if τ approach ξ_m^i. Here we design a new technique to calculate this integral precisely. We first rewrite the integral $\int_{t_{k-1}}^{t_k}(h_k^{j\prime}(\tau)/(\xi_m^i-\tau)^\alpha)d\tau$ into the form

$$\int_{t_{k-1}}^{t_k}\frac{h_k^{j\prime}(\tau)}{(\xi_m^i-\tau)^\alpha}d\tau = \frac{2^\alpha}{(t_k-t_{k-1})^\alpha}\int_{-1}^{1}\frac{h_j'(\theta)}{\left(\widetilde{\xi}_m^i-\theta\right)^\alpha}d\theta, \tag{18}$$

by the linear transformation

$$\tau = \frac{t_k-t_{k-1}}{2}\theta + \frac{t_k+t_{k-1}}{2}, \tag{19}$$

where $h_j'(\theta) = h_k^{j\prime}(\tau(\theta))$ is the Lagrangian polynomials based on the GLL points $x_j^{0,0}$, $j = 0, 1, \ldots, N$, and $\widetilde{\xi}_m^i = (2\xi_m^i - t_k - t_{k-1})/(t_k - t_{k-1})$. Next, we express h_j by the Legendre basis:

$$h_j(\theta) = \sum_{l=0}^{N}c_{jl}L_l(\theta), \tag{20}$$

where $c_{jl} = (L_l(\theta), h_j(\theta))/(L_l(\theta), L_l(\theta))$.

Now we turn to compute $\int_{-1}^{1}(L_l'(\theta)/(\widetilde{\xi}_m^i - \theta)^\alpha)d\theta$. By employing the property

$$\begin{aligned}L_l^{(p)}(1) &= \frac{1}{2^p}C_l^p\prod_{k=1}^{p}(l+k), \\ L_l^{(p)}(-1) &= (-1)^{l+p}\frac{1}{2^p}C_l^p\prod_{k=1}^{p}(l+k), \\ &\qquad p = 0, \ldots, l,\end{aligned} \tag{21}$$

and integrating $\int_{-1}^{1}(L_l'(\theta)/(\widetilde{\xi}_m^i - \theta)^\alpha)d\theta$ by parts, we get

$$\begin{aligned}&\int_{-1}^{1}\frac{L_l'(\theta)}{\left(\widetilde{\xi}_m^i-\theta\right)^\alpha}d\theta \\ &= -\sum_{p=1}^{l}\left[\frac{1}{2^p}C_l^p\prod_{k=1}^{p}\frac{l+k}{k-\alpha}\left(\widetilde{\xi}_m^i-1\right)^{p-\alpha}\right. \\ &\left.-(-1)^{l+p}\frac{1}{2^p}C_l^p\prod_{k=1}^{p}\frac{l+k}{k-\alpha}\left(\widetilde{\xi}_m^i+1\right)^{p-\alpha}\right].\end{aligned} \tag{22}$$

Thus, applying (18), (20), and (22) yields

$$\begin{aligned}B_{m,k}^1(i,j) &= -\frac{c(\alpha)2^\alpha}{(t_k-t_{k-1})^\alpha}\sum_{l=0}^{N}c_{jl}\int_{-1}^{1}\frac{L_l'(\theta)}{\left(\widetilde{\xi}_m^i-\theta\right)^\alpha}d\theta \\ &= \frac{c(\alpha)2^\alpha}{(t_k-t_{k-1})^\alpha} \\ &\cdot\sum_{l=0}^{N}c_{jl}\sum_{p=1}^{l}\left[\frac{1}{2^p}C_l^p\prod_{k=1}^{p}\frac{l+k}{k-\alpha}\left(\widetilde{\xi}_m^i-1\right)^{p-\alpha}\right. \\ &\left.-(-1)^{l+p}\frac{1}{2^p}C_l^p\prod_{k=1}^{p}\frac{l+k}{k-\alpha}\left(\widetilde{\xi}_m^i+1\right)^{p-\alpha}\right].\end{aligned} \tag{23}$$

Similarly, we can compute the matrices $B_{m,k}^2$ and $B_{m,k}^3$.

Equation (13) is a nonlinear nonsymmetric system. We use the Jacobian-free Newton-Krylov methods to solve it. Let $\mathbf{U}_m = (\mathbf{u}_m, \mathbf{v}_m, \mathbf{w}_m)^T$; we rewrite (13) in the following form: for $1 \le m \le M$,

$$\begin{aligned}F_1(\mathbf{U}_m) &= A_m^1\mathbf{u}_m + \sigma\mathbf{u}_m - \sigma\mathbf{v}_m - \sum_{k=1}^{m-1}B_{m,k}^1\mathbf{u}_k = \mathbf{0}, \\ F_2(\mathbf{U}_m) &= A_m^2\mathbf{v}_m - \rho\mathbf{u}_m + \mathbf{v}_m + \mathbf{u}_m * (\mathbf{w}_m)^r \\ &\quad - \sum_{k=1}^{m-1}B_{m,k}^2\mathbf{v}_k = \mathbf{0}, \\ F_3(\mathbf{U}_m) &= A_m^3\mathbf{w}_m + b\mathbf{w}_m - \mathbf{u}_m * \mathbf{v}_m - \sum_{k=1}^{m-1}B_{m,k}^1\mathbf{w}_k \\ &= \mathbf{0}.\end{aligned} \tag{24}$$

The iteration can be described as follows:

(i) The initial guess $\mathbf{U}_m^{(\mathbf{0})}$ is given.

(ii) Using BI-Conjugate-Gradient-stab (BICGstab) method solve the following linear system:

$$\mathcal{J}_{F_i}\left(\mathbf{U}_m^{(k)}\right)\delta\mathbf{U} = -F_i\left(\mathbf{U}_m^{(k)}\right), \tag{25}$$

where $\delta\mathbf{U} = (\delta\mathbf{u}, \delta\mathbf{v}, \delta\mathbf{w})^T$, k is the iteration index, and $\mathcal{J}_{F_i}(\mathbf{U}^{(k)})$ is the Jacobian matrix of function F_i at $\mathbf{U}_m^{(k)}$. We need not compute the matrix $\mathcal{J}_{F_i}(\mathbf{U}_m^{(k)})$. In fact, only the matrix-vector product is needed in the BICGstab method. Let $dF_i(\mathbf{U}_m^{(k)}, \delta\mathbf{U})$ be the Fréchet derivative of the function F_i at $\mathbf{U}_m^{(k)}$ with respect to the direction $\delta\mathbf{U}$. Consider

$$\begin{aligned}\mathcal{J}_{F_1}\left(\mathbf{U}_m^{(k)}\right)\delta\mathbf{U} &= \lim_{\varepsilon\to 0}\frac{F_1\left(\mathbf{U}^{(k)}+\varepsilon\delta\mathbf{U}\right)-F_1\left(\mathbf{U}^{(k)}\right)}{\varepsilon} \\ &= A_m^1\delta\mathbf{u} + \sigma\delta\mathbf{u} - \sigma\delta\mathbf{v}, \\ \mathcal{J}_{F_2}\left(\mathbf{U}_m^{(k)}\right)\delta\mathbf{U} &= \lim_{\varepsilon\to 0}\frac{F_2\left(\mathbf{U}_m^{(k)}+\varepsilon\delta\mathbf{U}\right)-F_2\left(\mathbf{U}_m^{(k)}\right)}{\varepsilon} \\ &= A_m^2\delta\mathbf{u} - \rho\delta\mathbf{u} + \delta\mathbf{v} + (\mathbf{w}_m)^r * \delta\mathbf{u} \\ &\quad + r\mathbf{u}_m * (\mathbf{w}_m)^{r-1} * \delta\mathbf{w},\end{aligned}$$

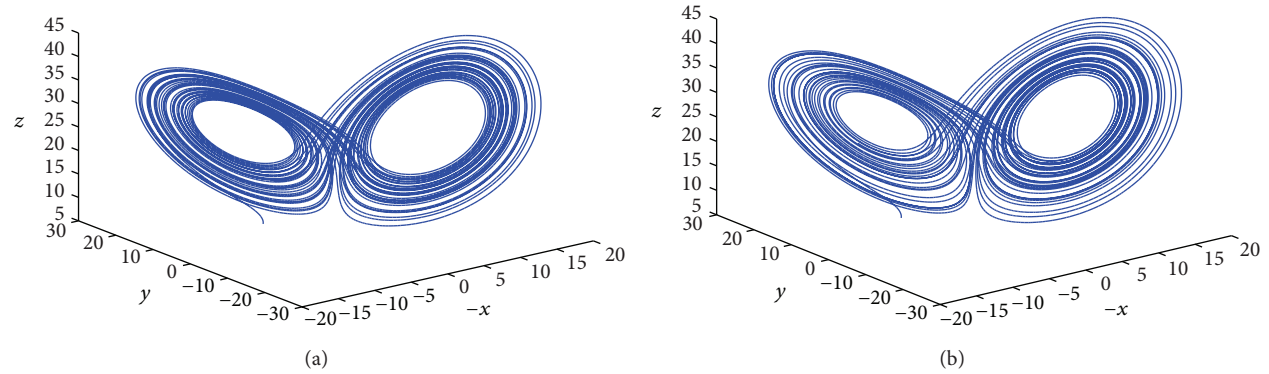

FIGURE 1: The phase portraits of x-y-z for fractional Lorenz system $\alpha = \beta = \gamma = 0.98$ (left) and $\alpha = \beta = \gamma = 0.99$ (right) for the case $r = 1$.

$$\begin{aligned}\mathcal{J}_{F_3}\left(\mathbf{U}_m^{(k)}\right)\delta\mathbf{w} &= dF_3\left(\mathbf{U}_m^{(k)}, \delta\mathbf{U}\right)\\ &= \lim_{\varepsilon\to 0}\frac{F_3\left(\mathbf{U}_m^{(k)} + \varepsilon\delta\mathbf{U}\right) - F_3\left(\mathbf{U}_m^{(k)}\right)}{\varepsilon}\\ &= A_m^3\delta\mathbf{w} + b\delta\mathbf{w} - \mathbf{u}_m * \delta\mathbf{v} - \mathbf{v}_m * \delta\mathbf{u}.\end{aligned} \tag{26}$$

(iii) Update $\mathbf{U}_m^{(k)}$ by

$$\mathbf{U}_m^{(k+1)} = \mathbf{U}_m^{(k)} + \omega \cdot \delta\mathbf{U}, \tag{27}$$

where ω is the correction factor, which is selected such that

$$\left\|F\left(\mathbf{U}_m^{(k+1)}\right)\right\| < (1 - \lambda\omega)\left\|F\left(\mathbf{U}_m^{(k)}\right)\right\|, \tag{28}$$

where $\lambda = 1/10$ is a scale parameter; we test $\omega = 1, 1/4, 1/16, \ldots$, until (28) is satisfied.

(iv) Stop the iteration, if

$$\frac{\|\delta\mathbf{U}\|}{\left\|\mathbf{U}_m^{(k)}\right\|} \le 10^{-15}. \tag{29}$$

3. Numerical Results

For a comparison with [2, 14], we take the initial values $x(0) = 10$, $y(0) = 0$, and $z(0) = 10$. In our numerical experiments, we take $T = 20$, $\Delta t = 0.004$, $\widetilde{N} = 1$, and $N = 5$.

First, we consider the case $\rho = 28$, $\sigma = 10$, $b = 8/3$, and $r = 1$. Note that, in this case, the equilibrium points of (3) are the origin, and

$$Q_\pm = \left(\pm 6\sqrt{2}, \pm 6\sqrt{2}, 27\right). \tag{30}$$

As pointed in [2], the solution can exhibit chaotic behavior if the effective dimension $\Sigma = \alpha + \beta + \gamma$ is greater than the critical dimension Σ_{cr}. In our numerical experiments, we take $\alpha = \beta = \gamma = 0.99$ and $\alpha = \beta = \gamma = 0.98$ and $\alpha = \beta = \gamma = 0.97$. The phase portraits of x, y, z are shown in Figures 1 and 2.

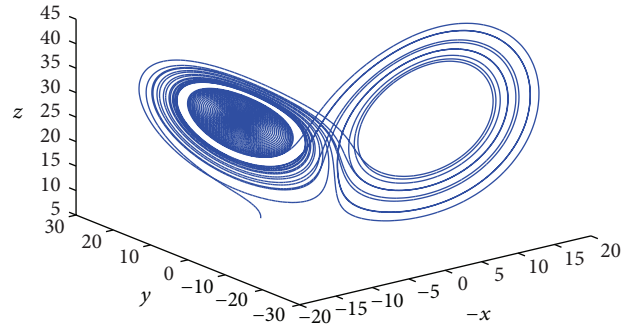

FIGURE 2: The phase portraits of x-y-z for fractional Lorenz system $\alpha = \beta = \gamma = 0.97$ for the case $r = 1$.

From these figures, it may be concluded that, for $\alpha = \beta = \gamma = 0.98$ up to $\alpha = \beta = \gamma = 1$, the system is chaotic, while for $\alpha = \beta = \gamma < 0.97$, the system turns to be regular and the solution converges to one of the two equilibrium points $Q_\pm$. This also coincides with other numerical results.

Secondly, we take $r = 2$, while other parameters ρ, σ and b are given above. Furthermore, we take $r = 3$, while other parameters ρ, σ and b are given above. The equilibrium points of (3) are the origin, and

$$Q_\pm = \left(\pm 2\sqrt{2\sqrt{3}}, \pm 2\sqrt{2\sqrt{3}}, 3\sqrt{3}\right). \tag{31}$$

The results are similar to the case of $r = 1$. However, the critical efficient dimension Σ_{cr} is much smaller than the case $r = 1$. From Figure 3, it may be concluded that, for $\alpha = \beta = \gamma = 0.94$ up to $\alpha = \beta = \gamma = 1$, the system is chaotic, while for $\alpha = \beta = \gamma < 0.93$, the system turns to be regular and the solution converges to one of the two equilibrium points $Q_\pm$.

Furthermore, if we take $r = 3$, while other parameter as given above. The equilibrium points are the origin, and

$$Q_\pm = \left(\pm 2\sqrt{2}, \pm 2\sqrt{2}, 3\right). \tag{32}$$

We can see from Figure 4 that the critical efficient dimension Σ_{cr} is much smaller than the case $r = 2$.

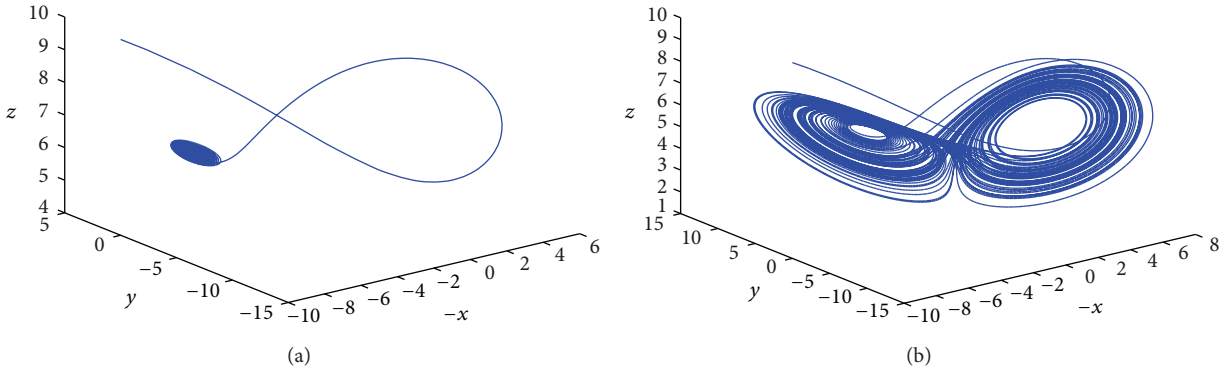

Figure 3: The phase portraits of x-y-z for fractional Lorenz systems $\alpha = \beta = \gamma = 0.93$ (left) and $\alpha = \beta = \gamma = 0.94$ (right) for the case $r = 2$.

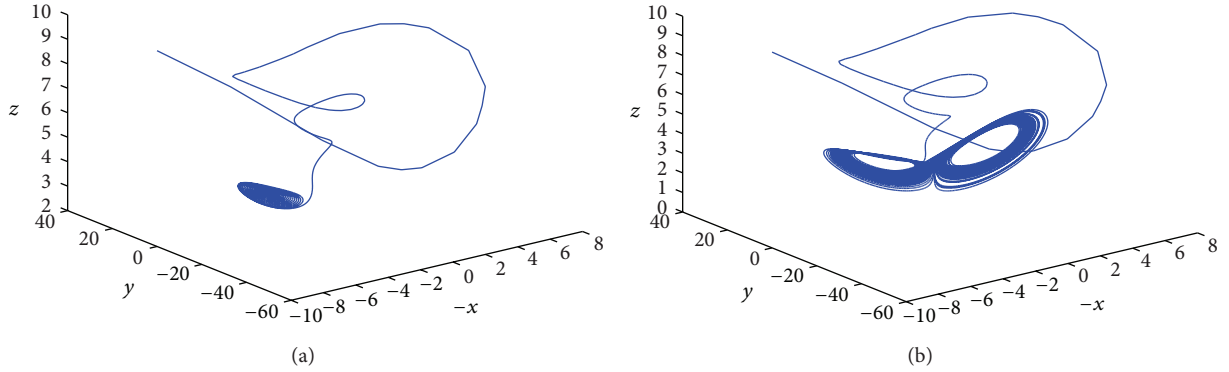

Figure 4: The phase portraits of x-y-z for fractional Lorenz systems $\alpha = \beta = \gamma = 0.91$ (left) and $\alpha = \beta = \gamma = 0.92$ (right) for the case $r = 3$.

Table 1: Comparison with FDM and FEM.

	Spectral method	FDM	FEM
Convergence rate	$O(e^{-cN})$	$\geq N^{\alpha-r}$	$\geq N^{-2}$
Complexity	$O(N^3)$	$O(N^3)$	$O(N^3)$
Storage	22	$O(10^9)$	$O(10^5)$

4. Efficiency of the Method

4.1. Comparison with Other Methods. In Table 1, we compare the spectral method with classical finite difference method and finite element method with respect to convergence rate, computational complexity, and storage.

Spectral method is well-known for its exponential convergency, that is, e^{-cN}, where N is the freedom of the discretized space. The convergence rate is slower than N^{-2} for finite element method [7, 12] and slower than $N^{\alpha-r}, r \leq 4$ for finite difference method [10, 17–20].

For partial differential equations of integral order, the final matrix is full for spectral method while sparse for both finite difference method and finite element method. Compared with spectral method, sparse matrix is the main advantage of finite difference method and finite element method for solving integral differential equations. However, for the fractional differential equations, the final matrix for all three methods is full. The presence of the integral in the noninteger order derivatives means that the solution at a time t_k depends on the solutions at all previous time levels $t < t_k$. This fact makes the final matrix full. So the computation complexity is about $O(N^3)$ with $O(N^2)$ for matrix-vector multiple and $O(N)$ for iteration steps.

Furthermore, all previous solutions have to be saved to compute the solution at the current time level which would make the storage very expensive if low-order methods are employed for temporal discretization. For example, we consider fractional ordinary differential equations:

$$
\begin{aligned}
{}_0D_t^{\alpha} x &= \sigma (y - x) + g_1(t), \\
{}_0D_t^{\beta} y &= \rho x - y - xz^r + g_2(t), \\
{}_0D_t^{\gamma} z &= xy - bz + g_3(t),
\end{aligned}
\tag{33}
$$

with $x(t) = y(t) = z(t) = \sin \pi t, t \in [0, 1]$. If 10^{-10} precision is desired, $\alpha = \beta = \gamma = 0.9$, then 22, $O(10^9)$, and $O(10^5)$ mounts of storage are used to approximate an exact solution by spectral method, finite difference method [10] ($r = 2$), and finite element method [12] ($r = 2$), respectively. In view of these three advantages, spectral method is the national choice for the fractional differential equation.

4.2. Efficiency of the Parallel Method. The parallelism efficiency is demonstrated by a cost comparison between

the parallel in time scheme and the classical sequential scheme based on the corresponding fine mesh.

First, the classical sequential scheme based on the fine mesh consists of solving the problems $\mathscr{F}_m(t, U_1, U_2, \ldots, U_{m-1})$ consecutively for $1 \le m \le M$. The computational complexity is equal to the sum of all the elementary operations:

$$\mathscr{C}_{\mathscr{F}} = \sum_{m=1}^{M} \mathscr{C}_{\mathscr{F}}^{n} = O\left(MN^3\right). \tag{34}$$

If we implement the scheme in a parallel architecture with enough processors, then the total computational time corresponds to the cost to solve a sequential set of M coarse subproblems and a fine subproblem in a single processor. If K is the number of iterations required to achieve the desired convergence of the parallel in time algorithm, then the total computational complexity is

$$K\left[\mathcal{O}\left(M\widetilde{N}^2 + NM\widetilde{N}\right) + \mathcal{O}\left(N^2\right) + \mathcal{O}\left(NM\widetilde{N}\right)\right]. \tag{35}$$

Comparing (34) with (35), we obtain a speed up (i.e., the percentage with respect to the sequential scheme) close to

$$\mathcal{O}\left(K\frac{\widetilde{N}^2}{N^3} + K\frac{\widetilde{N}}{N^2} + \frac{K}{NM}\right)^{-1}. \tag{36}$$

Conflict of Interests

The author declares that there is no conflict of interests regarding the publication of this paper.

Acknowledgments

The author is very thankful to the anonymous referees, who carefully read through the paper and made helpful suggestions that have significantly improved the presentation of this paper. This work was partially supported by National NSF of China (11226081) and NSF of Fujian Province (2013J05003).

References

[1] E. N. Lorenz, "Deterministic nonperiodic flow," *Journal of the Atmospheric Sciences*, vol. 20, pp. 130–142, 1963.

[2] I. Grigorenko and E. Grigorenko, "Chaotic dynamics of the fractional Lorenz system," *Physical Review Letters*, vol. 91, no. 3, Article ID 034101, pp. 214–217, 2003.

[3] R. Metzler and J. Klafter, "The random walk's guide to anomalous diffusion: a fractional dynamics approach," *Physics Reports*, vol. 339, no. 1, pp. 1–77, 2000.

[4] D. del-Castillo-Negrete, B. A. Carreras, and V. E. Lynch, "Front dynamics in reaction-diffusion systems with Levy flights: a fractional diffusion approach," *Physical Review Letters*, vol. 91, no. 1, Article ID 018302, 2003.

[5] R. Gorenflo, F. Mainardi, D. Moretti, and P. Paradisi, "Time fractional diffusion: a discrete random walk approach," *Nonlinear Dynamics*, vol. 29, no. 1–4, pp. 129–143, 2002.

[6] K. M. Kolwankar and A. D. Gangal, "Local fractional Fokker-Planck equation," *Physical Review Letters*, vol. 80, no. 2, pp. 214–217, 1998.

[7] V. J. Ervin and J. P. Roop, "Variational formulation for the stationary fractional advection dispersion equation," *Numerical Methods for Partial Differential Equations*, vol. 22, no. 3, pp. 558–576, 2006.

[8] X. J. Li and C. J. Xu, "A space-time spectral method for the time fractional diffusion equation," *SIAM Journal on Numerical Analysis*, vol. 47, no. 3, pp. 2108–2131, 2009.

[9] X. J. Li and C. J. Xu, "Existence and uniqueness of the weak solution of the space-time fractional diffusion equation and a spectral method approximation," *Communications in Computational Physics*, vol. 8, no. 5, pp. 1016–1051, 2010.

[10] Y. M. Lin and C. J. Xu, "Finite difference/spectral approximation for the time fractional diffusion equations," *Journal of Computational Physics*, vol. 2, no. 3, pp. 1533–1552, 2007.

[11] F. Liu, V. V. Anh, I. Turner, and P. Zhuang, "Time fractional advection-dispersion equation," *Journal of Applied Mathematics & Computing*, vol. 13, no. 1-2, pp. 233–245, 2003.

[12] J. P. Roop, "Computational aspects of FEM approximation of fractional advection dispersion equations on bounded domains in $\mathbb{R}^2$," *Journal of Computational and Applied Mathematics*, vol. 193, no. 1, pp. 243–268, 2006.

[13] W. Wyss, "The fractional diffusion equation," *Journal of Mathematical Physics*, vol. 27, no. 11, pp. 2782–2785, 1986.

[14] A. K. Alomari, M. S. M. Noorani, R. Nazar, and C. P. Li, "Homotopy analysis method for solving fractional Lorenz system," *Communications in Nonlinear Science and Numerical Simulation*, vol. 15, no. 7, pp. 1864–1872, 2010.

[15] M. S. H. Chowdhury, I. Hashim, and S. Momani, "The multistage homopoty-perturbation method: a powerful scheme for handling the Lorenz system," *Communications in Nonlinear Science and Numerical Simulation*, vol. 15, pp. 1864–1872, 2010.

[16] X. J. Li, T. Tang, and C. J. Xu, "Parallel in time algorithm with spectral-subdomain enhancement for Volterra integral equations," *SIAM Journal on Numerical Analysis*, vol. 51, no. 3, pp. 1735–1756, 2013.

[17] W. H. Deng, "Finite element method for the space and time fractional Fokker-Planck equation," *SIAM Journal on Numerical Analysis*, vol. 47, no. 1, pp. 204–226, 2008/09.

[18] M. H. Chen and W. H. Deng, "High order algorithms for the fractional substantial diffusion equation with truncated Lévy flights," *SIAM Journal on Scientific Computing*, vol. 37, no. 2, pp. 890–917, 2015.

[19] L. J. Zhao and W. H. Deng, "A series of high order quasi-compact schemes for space fractional diffusion equations based on the superconvergent approximations for fractional derivatives," Numerical Methods for Partial Differential Equations, http://arxiv.org/abs/1312.7069.

[20] L. J. Zhao and W. H. Deng, "High order finite difference methods on non-uniform meshes for space fractional operators," http://arxiv.org/abs/1412.4339.

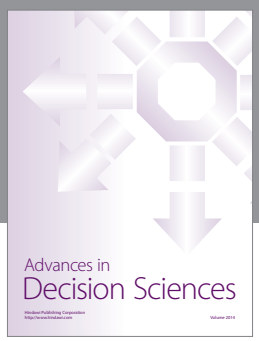

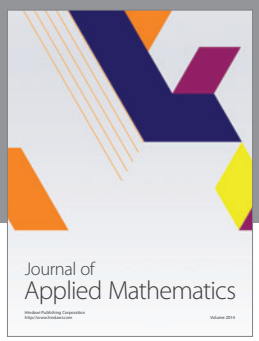

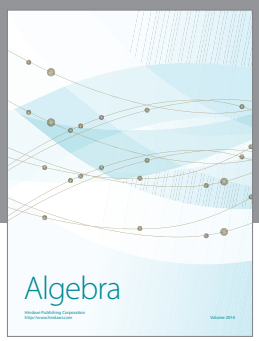

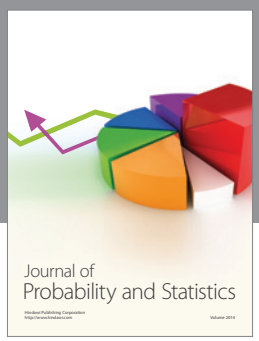

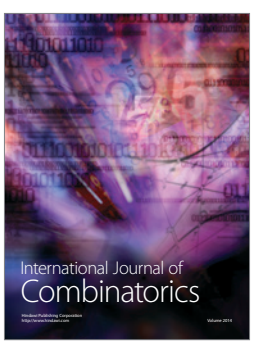

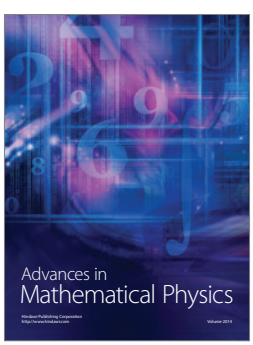

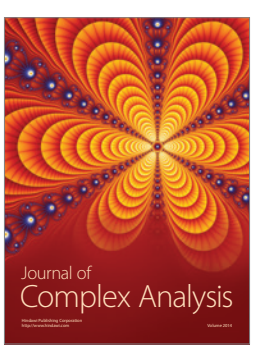

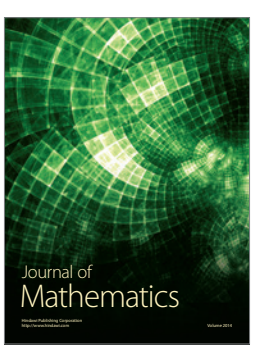

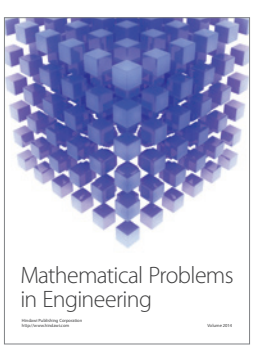

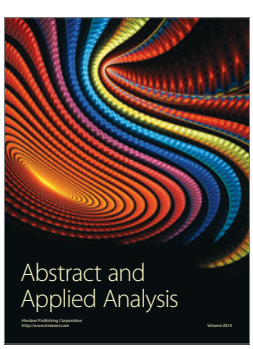

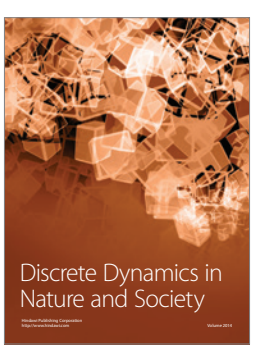

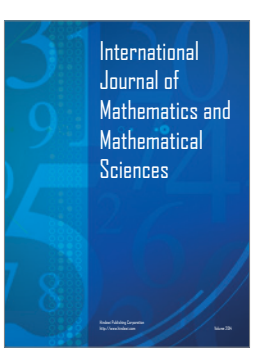

Hindawi

Submit your manuscripts at
http://www.hindawi.com